Isospin transport at Fermi energies

V. Baran,[1,2] M. Colonna,[1] M. Di Toro,[1] M. Zielinska-Pfabé,[3] and H. H. Wolter[4]
[1]*Laboratori Nazionali del Sud, Via S. Sofia 44, and Physics-Astronomy Department, University of Catania, I-95123 Catania, Italy*
[2]*NIPNE-HH, Bucharest and Bucharest University, Romania*
[3]*Smith College, Northampton, Massachusetts 01063, USA*
[4]*Physics Department, University of Munich, D-85748 Garching, Germany*
(Received 28 June 2005; revised manuscript received 27 September 2005; published 30 December 2005)

In this paper we investigate isospin transport mechanisms in semiperipheral collisions at Fermi energies. The effects of the formation of a low density region (neck) between the two reaction partners and of preequilibrium emission on the dynamics of isospin equilibration are carefully analyzed. We clearly identify two main contributions to the isospin transport: isospin diffusion due to the N/Z ratio and isospin drift due to the density gradients. Both effects are sensitive to the symmetry part of the nuclear equation of state (EOS), in particular to the value and slope around saturation density.

DOI: 10.1103/PhysRevC.72.064620 PACS number(s): 25.70.Lm, 25.70.Pq

I. INTRODUCTION

In the last few years the increased accuracy of the experimental techniques has renewed interest in nuclear reactions at Fermi energies. Exclusive measurements, event-by-event analysis, and a 4π coverage allow a deeper investigation of the evolution of the reaction mechanisms with beam energy and centrality. New insights into the understanding of the nuclear matter equation-of-state (EOS) were gained [1]. In particular, recent experimental and theoretical analyses were devoted to the study of the properties and effects of the symmetry term of the EOS (asy-EOS) away from saturation conditions [2,3].

Indeed, the two-component character of nuclear matter adds some special interest to the dynamics of heavy ion collisions at intermediate energies, between 20 and 100A MeV. In *central* collisions isospin distillation is an important effect in multifragmentation of charge asymmetric systems. Here phase separation is driven by isoscalar-like unstable fluctuations, i.e., local in phase variations of proton and neutron densities [4–7]. This leads to a more symmetric "liquid" phase of fragments surrounded by a more neutron rich "gas" relative to the original asymmetry of the system. Isoscaling phenomena, observed experimentally, provide indications for such a scenario [8,9].

In *semiperipheral* collisions between nuclei with different N/Z ratio, isospin dynamics will drive the system toward a uniform asymmetry distribution. The degree of equilibration, correlated to the interaction time, should provide some insights into transport properties of fermionic systems [10,11], in particular give information on transport coefficients of asymmetric nuclear matter [12,13].

The aim of this work is to investigate the isospin transfer through the neck region in semiperipheral collisions of asymmetric nuclei at Fermi energies. The isospin transfer was measured for collisions of different Sn isotopes at MSU [14–16] and interpreted theoretically with the result that the asy-EOS should be rather stiff. In these works the effect of preequilibrium emission, which changes the isospin content of the interacting system, was not analyzed explicitly. Here we will discuss this questions in detail, as well as the different transport processes affecting the final isospin content. Of particular interest is the role of the density dependence of the symmetry energy. Finally an analytical evaluation of the isospin transport properties will clearly show the relation between diffusion and drift coefficients to value and slope of the symmetry energy, respectively. This is very important for a direct understanding of the simulation results, as well as for planning experiments aimed to get independent information on the symmetry energy and its density dependence below the equilibrium value. Quantitatively, dynamical isospin effects can be properly understood only from microscopic calculations based on transport models. We will base our study on a stochastic BNV transport model (see Refs. [17,18] for more details on the main ingredients of this approach).

II. ISOSPIN EQUILIBRATION PROCESS

We are focusing on the charge asymmetric collision $^{124}\mathrm{Sn} + {}^{112}\mathrm{Sn}$, at 50$A$ MeV bombarding energy, to which we refer as the mixed system, (M). To investigate the density (ρ) dependence we consider here two representative parameterizations of the symmetry energy, $E_{\mathrm{sym}}(\rho, I)/A \equiv C_{\mathrm{sym}}(\rho)I^2$, $I \equiv (N - Z)/A$: One showing a rapidly increasing behavior with density, roughly proportional to ρ^2 (asysuperstiff) and one where a kind of saturation is observed above normal density (asysoft, SKM*) (see Refs. [3,6] for more detail).

The BNV simulations have been performed for semiperipheral collisions at impact parameters $b = 6, 8, 9, 10$ fm. In the last two cases the reaction has dominantly a binary character and the charge asymmetry of primary projectile (target)-like fragments, PLF (TLF), should provide the essential information about the isospin equilibration rate. At $b = 8$ fm already about 25% of the events are ternary. An intermediate mass fragment (IMF) can be formed in the midvelocity region by neck fragmentation [19]. For more central events this mechanism becomes dominant: at $b = 6$ fm, one or two IMF's are found in more than 70% of events [6]. The fragment formation in the neck region could influence the final isospin distribution of the PLF/TLF, so in the following we will

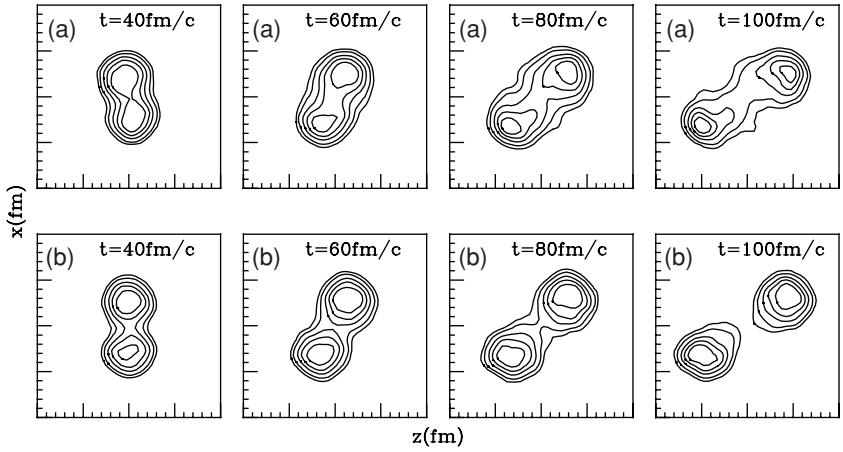

FIG. 1. ^{124}Sn + ^{112}Sn $b = 8$ fm (upper row) and $b = 10$ fm (lower row) collision: density contour plots. The side of each box is 40 fm.

discuss isospin equilibration in binary as well as in ternary events. We define the average interaction time, t_c, as the time elapsed between the initial touching and the moment when PLF and TLF reseparate. From our simulations we obtain $t_c \approx 140, 120, 100, 80\,\mathrm{fm}/c$ for the impact parameters $b = 6, 8, 9, 10$ fm, respectively. 400 events were calculated for each initial condition and for each asy-EOS.

Typical density contour plots, at $b = 8$ fm and $b = 10$ fm, are shown in Fig. 1. We note the dynamical evolution of the overlap region: driven by the fast leading motion of PL- and TL-prefragments, the formation of a lower density interface can be clearly observed after around $40\,\mathrm{fm}/c$.

An isospin migration, or transport, takes place during this transient configuration of two residues with densities close to the normal one, separated by a dilute neck region. This is the new qualitative feature of the charge equilibration dynamics at the Fermi energies, due to the interplay between concentration (N/Z content) and density gradients. In contrast, in deep-inelastic collisions at lower energies the isospin equilibration is only driven by the N/Z difference between the interacting nuclei having a quite uniform density profile without a low density interface until separation [20].

We remind the reader that density gradients induce isospin transport through the density variation of proton/neutron chemical potentials $\mu_{p/n}$ [3]. Since $\mu_n - \mu_p = 4C_{\mathrm{sym}}(\rho)I$, where $I = (N - Z)/A$, from an accurate study of isospin equilibration at Fermi energies we expect to get independent information on the slope of the symmetry energy below saturation density. This point will be carefully elaborated in Sec. IV.

We quantify the degree of equilibration by the isospin transport (imbalance) ratio [21], defined as

$$R_i = \frac{2I_i^M - I_i^H - I_i^L}{I_i^H - I_i^L}. \qquad (1)$$

Here $i = P, T$ stands for the projectile-like (target-like) fragment. The quantities I_i refer to the asymmetry or in general to any isospin dependent quantity, characterizing the fragments at separation time, for the mixed reaction (M, 124 + 112), the reactions between neutron rich (H, 124 + 124), and between neutron poor nuclei (L, 112 + 112), respectively. A value of R_i approaching zero is an indication of a large degree of equilibration. The extreme cases $R_T = -1$ and $R_P = 1$ correspond to the absence of any isospin transfer.

The results of the calculations are shown in Fig. 2 for the dependence of $R_{P/T}$ on the interaction time t_c for the asysoft (squares) and asysuperstiff (circles) EOS's. The figure also shows the experimental values extracted in Refs. [15,16] at semiperipheral collisions at about $b = 8$ fm. The points on the figure are obtained considering only binary events. However, from the analysis of ternary events, where an IMF comes out of the neck region, we obtain essentially the same values, as the ones displayed in Fig. 2, for the PLF and TLF imbalance ratio. Due to the neutron enrichment of the neck region [6], the IMF emission reduces the asymmetry of the remaining system. However this happens in the three reactions considered (M, H, and L) and, as a matter of fact, it does not affect much the rate of isospin equilibration between PLF and TLF, as measured through the imbalance ratio.

It might be interesting to calculate the imbalance ratio also for the IMF coming from the neck region, in ternary events. This is also shown in Fig. 2 (triangles) for $b = 6, 8$ fm. The imbalance ratio is almost zero for both asy-EOS, indicating

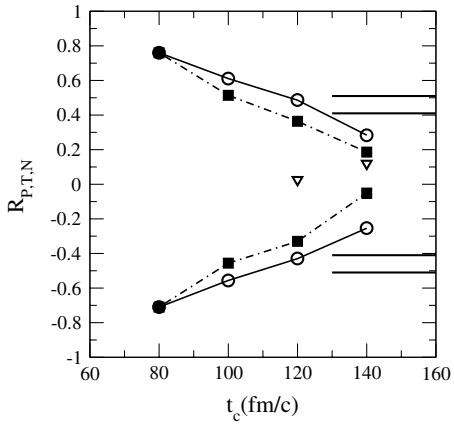

FIG. 2. The isospin transport ratio $R_{P,T}$, Eq. (1), for the asysoft (full squares) and asysuperstiff (circles) EOS's as a function of the interaction time t_c, corresponding to different impact parameter b. The band between the two solid lines corresponds to the experimental data of Refs. [15,16]. The triangles represent the imbalance ratio calculated for the neck fragments, in ternary events.

that the asymmetry of the neck region in the M reaction can be considered as the average of the values obtained in the H and L reactions. This is not an obvious result because, due to preequilibrium effects and to the neutron enrichment, the isotopic content of the neck region is not trivially connected to the initial asymmetry of the composite system.

R_{PT} exhibits a nearly linear behavior with respect to the interaction time, with a slight change of the slope (of about 15%) between the two equations of state. The smaller values of isospin transport ratios for the asysoft EOS point toward a faster equilibration rate. In Refs. [15,22] an explanation was based on the observation that below normal density the asysoft EOS has a larger value of the symmetry energy. Therefore an enhanced isospin equilibration will occur if the diffusion takes place at uniform lower density. We intend to show that in fact the mechanism of charge equilibration is more complicated due to the dynamical evolution of the reaction at these energies. Fast particle emission and density gradients, due to the development of the low-density interface between PLF and TLF, will also play a role.

In the next section we investigate more in detail the influence of the various processes, focusing on binary reactions.

III. ISOSPIN SHARING AT FERMI ENERGIES

The isospin content of the two residues in a mixed collision system at separation time is determined by the interplay between the particle emission to the gas from each nucleus during the overlap and the transfer of nucleons through the neck. We thus write simple balance equations:

$$I_P = \frac{A_P^0}{A_P}\left(I_P^0 - \frac{A_{gP}}{A_P^0}I_{gP} - \frac{A_{PT}}{A_P^0}I_{PT} + \frac{A_{TP}}{A_P^0}I_{TP}\right), \quad (2)$$

$$I_T = \frac{A_T^0}{A_T}\left(I_T^0 - \frac{A_{gT}}{A_T^0}I_{gT} + \frac{A_{PT}}{A_T^0}I_{PT} - \frac{A_{TP}}{A_T^0}I_{TP}\right). \quad (3)$$

Here I_P (I_T) and A_P (A_T) are the PLF (TLF) asymmetry and mass at separation, I_P^0 (I_T^0) and A_P^0 (A_T^0) the initial projectile (target) asymmetry and mass. Then I_{gP} (I_{gT}), A_{gP} (A_{gT}) are the asymmetries and masses of the projectile/target "gas", i.e., of the preequilibrium particles emitted by the projectile (target) during the interaction time. Finally I_{PT} (I_{TP}), and A_{PT} (A_{TP}) are the asymmetry and mass of all nucleons transferred from projectile (target) to target (projectile).

Exploiting Eqs. (2) and (3), it is possible to estimate the effect of isospin transport and preequilibrium emission on the imbalance ratio. Within the following approximations:

$$\left.\frac{A_P^0}{A_P}\right|_M \approx \left.\frac{A_P^0}{A_P}\right|_H \approx \left.\frac{A_P^0}{A_P}\right|_L; \quad \left.\frac{A_{gP}}{A_P^0}\right|_M \approx \left.\frac{A_{gP}}{A_P^0}\right|_H \approx \left.\frac{A_{gP}}{A_P^0}\right|_L; \quad (4)$$

$$A_{TP} \approx A_{PT}; \quad I_{gP}^M \approx I_{gP}^H; \quad I_{gT}^M \approx I_{gT}^L, \quad (5)$$

where the indices M, H, L refer again to the mixed (124 + 112), the neutron rich (124 + 124) and the neutron deficient (112 + 112) systems, we arrive at a simplified expression for the isospin transport ratio for the projectile which shows explicitely the dependence on the isospin transport ($I_{PT} - I_{TP}$) and on the pre-equilibrium emission ($I_{gP}^H - I_{gP}^L$):

$$R_P \approx 1 - \frac{2\frac{A_{PT}}{A_P^{0,H}}(I_{PT} - I_{TP})}{I_P^{0,H} - I_P^{0,L} - \frac{A_{gP}}{A_P^{0,H}}\left(I_{gP}^H - I_{gP}^L\right)}. \quad (6)$$

With similar approximations the target isospin transport ratio can be expressed as

$$R_T \approx -1 + \frac{2\frac{A_{PT}}{A_T^{0,L}}(I_{PT} - I_{TP})}{I_T^{0,H} - I_T^{0,L} - \frac{A_{gT}}{A_T^{0,L}}\left(I_{gT}^H - I_{gT}^L\right)}. \quad (7)$$

We have checked that the approximated formulas (6), (7) reproduce the actual values of R_{PT}, Eq. (1), within 5%. Eqs. (6) and (7) clearly show that the transport ratios depend on the difference $I_{PT} - I_{TP}$, as expected, but also on the preequilibrium emission, which reduces their absolute value.

We now discuss how isospin transport and preequilibrium emission depend on the asy-EOS. In Fig. 3 we present the quantities I_{gP}, I_{gT} and A_{gP}, A_{gT}, as a function of the interaction time t_c, for the asysoft and the asysuperstiff EOS. We note that I_{gP} is much larger than I_P^0 and increases in more peripheral reactions, due to neutron skin effects. The same is true for the target but the difference is smaller. Thus the pre-equilibrium emission reduces the N/Z difference between the two nuclei, competing with the transfer process.

Comparing the results for the two EOS's we see that, for the most dissipative collisions, the asymmetry of preequilibrium emission is larger (by about 20%) in the asysoft case. Indeed, below normal density, from where most of the emitted nucleons originate, the neutrons (protons) are less (more)

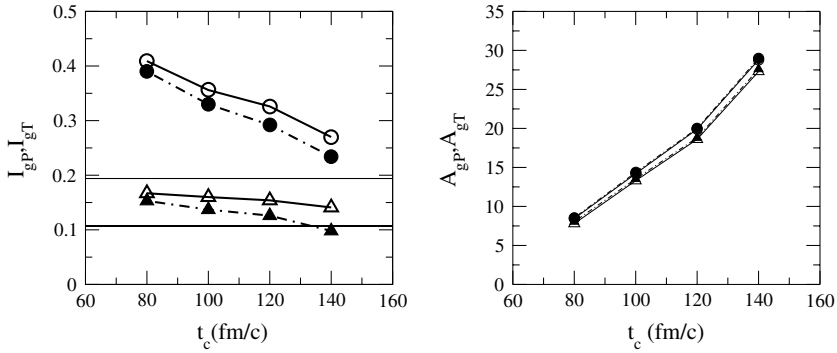

FIG. 3. ^{124}Sn + ^{112}Sn collision at 50A MeV: Isospin content and mass of preequilibrium particles I_{gP}, A_{gP} (I_{gT}, A_{gT}) emitted from the projectile (circles) (respectively, target, triangles), as a function of the interaction time t_c. Full symbols refer to asysuperstiff EOS, while open symbols represent asysoft calculations. The horizontal lines indicate the initial projectile and target asymmetries.

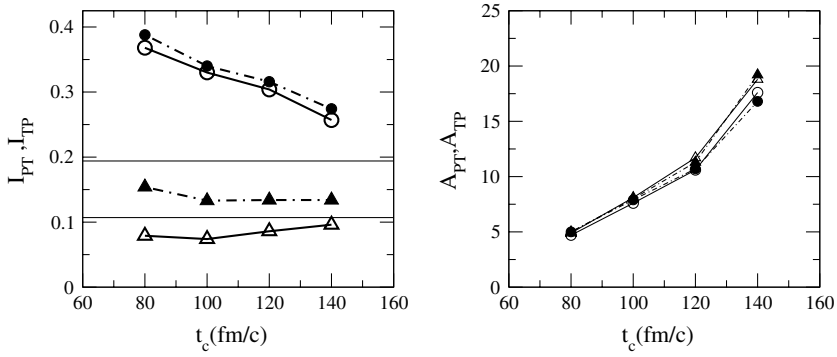

FIG. 4. Isospin content and mass of particles transferred from projectile(target) to target(projectile), I_{PT}, A_{PT} (I_{TP}, A_{TP}), as a function of t_c. Symbols are as in Fig. 3.

bound than for the asysuperstiff EOS. However, the differences between the two asy-EOS's are reduced at larger impact parameters, as seen in the results for $t_c = 80\,\mathrm{fm}/c$ ($b = 10\,\mathrm{fm}$), since the interaction times are much shorter. The total number of emitted nucleons is not very sensitive to the asy-EOS.

We next show in Fig. 4 the dependence of $I_{PT}(I_{TP})$ and $A_{PT}(A_{TP})$ on interaction time, i.e., impact parameter. We find a clear dependence on the asy-EOS of the isospin transferred between the two nuclei. Indeed we observe that

$$I_{PT}^{(\mathrm{asysuperstiff})} > I_{PT}^{(\mathrm{asysoft})} > I_P^0 = 0.192, \tag{8}$$

$$I_{TP}^{(\mathrm{asysuperstiff})} > I_T^0 = 0.107 > I_{TP}^{(\mathrm{asysoft})}. \tag{9}$$

We will show in the next chapter that the origin of these inequalities lies in the existence of the low density interface and the density dependence of symmetry energy. The asysuperstiff EOS favors the neutron migration toward the neck region from both participants. This explains why simultaneously $I_{PT}^{(\mathrm{asysuperstiff})} > I_P^0$ and $I_{TP}^{(\mathrm{asysuperstiff})} > I_T^0$. We will see that for the asysoft EOS this effect is weakened.

In Fig.5 we show the final asymmetry and mass of PLF and TLF. For the projectile, that is neutron rich, both preequilibrium emission and nucleon transfer drive the system toward a more symmetric configuration. The two processes have opposite effects and thus tend to compensate for the target. Therefore the projectile asymmetry has a more pronounced deviation from the corresponding initial value in comparison to the target. The amount of isospin equilibration between PLF and TLF increases with increasing t_c, as expected, and is larger for the asysoft EOS. On the basis of Eqs. (6) and (7) this can be simply understood in terms of the difference $I_{PT} - I_{TP}$ and of the isotopic content of the preequilibrium emission. Indeed both effects are larger in the asysoft case, as shown in Figs. 3 and 4. From Eqs. (6) and (7), one can easily see that this leads to smaller values of the imbalance ratio R_{PT}.

In the next chapter we investigate more in detail the relationship between the results discussed above and the properties of the EOS.

IV. INTERPRETATION OF THE RESULTS

The role of the EOS in isospin transport mechanims can be made more explicit by studying the response of nuclear matter, in the presence of neutron and proton density gradients. Since we are facing situations where local thermal equilibrium is reached, we will perform this study within the hydrodynamic limit, that makes the derivation of the isospin transport coefficients more transparent.

In such a framework the proton and neutron migration is dictated by the spatial gradients of the corresponding chemical potentials $\mu_{p/n}(\rho_p, \rho_n, T)$, where ρ_p and ρ_n are proton and neutron density and T denotes the temperature [3,23]. The currents of the two species can be expressed, in terms of the total density $\rho = \rho_n + \rho_p$ and $I = (\rho_n - \rho_p)/\rho$, as follows:

$$j_n = D_n^\rho \nabla\rho - D_n^I \nabla I, \tag{10}$$

$$j_p = D_p^\rho \nabla\rho - D_p^I \nabla I, \tag{11}$$

where D_q^ρ and D_q^I are drift and diffusion coefficients due to density and isospin gradients, respectively:

$$D_q^\rho = ct \left(\frac{\partial \mu_q}{\partial \rho}\right)_{I,T} \tag{12}$$

$$D_q^I = -ct \left(\frac{\partial \mu_q}{\partial I}\right)_{\rho,T}, \quad (q = n, p) \tag{13}$$

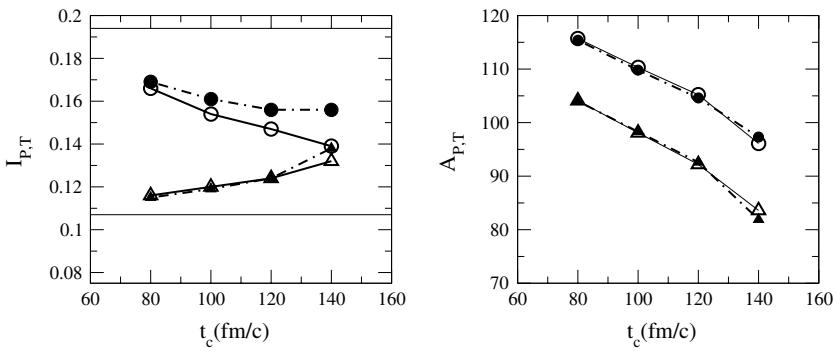

FIG. 5. Iospin content and mass of PLF and TLF, as a function of t_c. Symbols are as in Figs. 3 and 4.

(ct is a negative constant).

They can be expressed as

$$D_q^\rho = ct\left[N^{-1} + \frac{\partial U}{\partial \rho} \pm 2I\frac{\partial C_{\rm sym}}{\partial \rho} + O(I^2)\right] \quad (14)$$

$$D_q^I = \pm 2ct\ \rho\left[C_{\rm sym} \pm I\left(\rho\frac{\partial C_{\rm sym}}{\partial \rho} - C_{\rm sym}\right)\right] \quad (15)$$

$$(+n, -p),$$

where N^{-1} is the level density of symmetric matter at the same density and temperature and $U(\rho)$ is the isoscalar part of the mean-field potential.

One can see that the isovector part of the nuclear interaction enters the coefficients D_q^ρ through the derivative of the total symmetry energy $C_{\rm sym}$. On the other hand the isospin diffusion coefficients D_q^I depend, in leading order, on the value of the symmetry energy coefficient $C_{\rm sym}$. Moreover, it appears that the difference of neutron and proton drift coefficients, $D_n^\rho - D_p^\rho = \frac{\partial(\mu_n - \mu_p)}{\partial \rho}$, is equal to $4I\frac{\partial C_{\rm sym}}{\partial \rho}$, as one can simply derive also from the relation $\mu_n - \mu_p = 4C_{\rm sym}I$.

Various particular situations can be derived from these relations. In symmetric nuclear matter $D_n^I = -D_p^I$ and $D_n^\rho = D_p^\rho$. In the absence of density gradients the proton current will flow oppositely and equal in magnitude to the neutron current. On the other hand, for density gradients only, in asymmetric nuclear matter the proton and neutron currents may have the same direction but assume different values, inducing isospin gradients [24]. Such a situation can be encountered in semiperipheral collisions between identical, charge asymmetric nuclei with the formation of a dilute intermediate region [25].

For the two asy-EOS's we calculate the coefficients $D_q^i, i = \rho, I$ and $q = n, p$. We plot the ratios $R_q^i = D_q^{i,\rm asysuperstiff}/D_q^{i,\rm asysoft}$ in Fig. 6 as a function of the density for a fixed asymmetry $I = 0.2$. These values of the asymmetry and density are close to the physical conditions expected for the projectile or target region. The only negative coefficient is D_p^I. The isospin gradients, directed from the projectile to the neck and from the neck to the target, induce neutron and proton flows in opposite directions. However the ratios of the corresponding coefficients are quite close to unity for the two asy-EOS's and therefore the effects are similar.

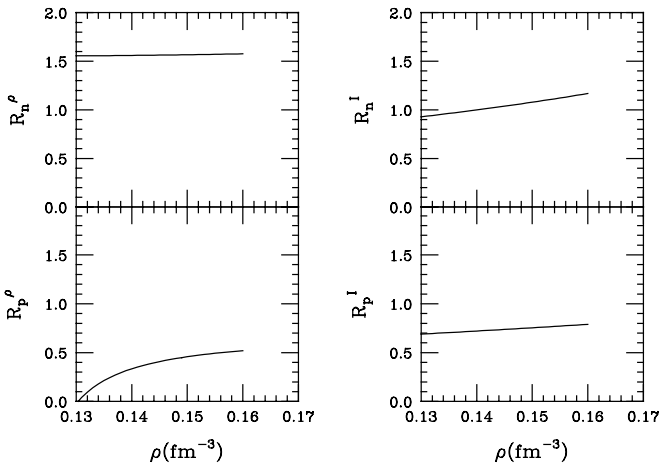

FIG. 6. Ratios of drift coefficients $R_q^i = D_q^{i,\rm asysuperstiff}/D_q^{i,\rm asysoft}$, $i = \rho, I$ and $q = n, p$, as a function of the density for fixed asymmetry $I = 0.2$.

Since the density gradient is oriented from projectile and target residues to the neck, neutrons and protons migrate from higher toward lower density regions. Around and below saturation density $R_n^\rho = D_n^{\rho,\rm asysuperstiff}/D_n^{\rho,\rm asysoft} > 1$ and $R_p^\rho = D_p^{\rho,\rm asysuperstiff}/D_p^{\rho,\rm asysoft} < 1$. These inequalities suggest that more neutrons and less protons migrate from projectile toward neck in the case of asysuperstiff EOS resulting in the formation of a more neutron rich intermediate region. This is due to the larger value of the derivative of the symmetry energy around normal density and is in agreement with the behavior observed in the numerical simulations, see Eqs. (8) and (9).

We note that for asysuperstiff EOS, in spite of an enhanced isospin migration toward the neck at separation time, the projectile residue is more asymmetric in comparison to the asysoft case. One reason is that for the asysuperstiff EOS during the preequilibrium emission not as many neutrons are removed as for the asysoft EOS. Also, as it was shown, for the asysuperstiff EOS more asymmetric matter is also transferred from the target.

V. CONCLUSIONS

In this work we have studied in detail processes related to isospin equilibration in semipheripheral collisions at Fermi energies and their dependence on the symmetry term of the EOS. A special feature of these reactions is the development of a low density interface between the two residues. The neck region is controlling the proton and neutron currents and their direction. The presence of density gradients also affects the isospin exchange between projectile and target and we have shown that this is sensitive to the density dependence of the symmetry energy. The neutron to proton ratio emitted during the interaction stage is also influenced by the asy-EOS. The interplay between the two processes leads to a stronger equilibration for asy-soft EOS, as it is evidenced by the isospin transport (imbalance) ratio. Actually, in the asy-stiff case, a larger isospin transfer is observed, due to the presence of density gradients, directed from PLF and TLF towards the neck region. However, finally we observe a kind of compensation between the asymmetry of the matter transferred from projectile to target (I_{PT}) and from target to projectile (I_{TP}). From this point of view, to put in better evidence effects due to the presence of density gradients, it would be more appropriate to study events where fragments originating from the neck region are also detected, with their isospin content. According to our simulations, fragment emission from the neck region reduces the asymmetry of PLF and TLF, but it does not affect much the degree of isospin equilibration, as defined by the imbalance ratio, Eq. (1). From this point of view, the imbalance ratio appears as a robust measure of isospin equilibration between the two collision partners, independently of the binary or ternary character of the reaction. However, as shown in Sec. III, results are sensitive to the amount and isotopic content of preequilibrium emission. Hence it should be noticed that, when performing

the comparison with experimental data, where the imbalance ratios are deduced from the isoscaling parameters of light fragments [15], some uncertainties may derive from the use of different isospin dependent observables, namely the N/Z of PLF and TLF, as reconstructed with the BNV procedure.

It would also be important to investigate the interplay between the effects due to the isoscalar and isovector part of the EOS on isospin transport observables. Indeed, more recent work, which considers momentum dependent interactions, has shown that the more repulsive character of the overall dynamics may reduce the symmetry energy stiffness required to reproduce the data [22].

In conclusion, charge equilibration measurements in semiperipheral heavy ion collisions at Fermi energies provide new independent observables to study the poorly known density dependence of the symmetry term of the nuclear EOS below saturation. This is of interest for other properties of asymmetric matter, like neutron skin and isovector collective response in finite nuclei, and may also be important for neutron star crust structures [3].

[1] P. Danielewicz, R. Lacey, and W. C. Lynch, Science **298**, 1592 (2002).

[2] *Isospin Physics in Heavy Ion Collisions at Intermediate Energies*, edited by Bao-An Li and W. Udo Schroeder (NOVA Science Publishers, Inc., New York, 2001).

[3] V. Baran, M. Colonna, V. Greco, and M. Di Toro, Phys. Rep. **410**, 235 (2005).

[4] V. Baran, M. B. Tsang, W. A. Friedman, C. K. Gelbke, W. G. Lynch, G. Verde, and H. Xu, Phys. Rev. Lett. **86**, 5023 (2001).

[5] M. Colonna, P. Chomaz, and S. Ayik, Phys. Rev. Lett. **88**, 122701 (2002).

[6] V. Baran *et al.*, Nucl. Phys. **A703**, 603 (2002).

[7] J. Margueron and Ph. Chomaz, Phys. Rev. C **67**, 041602(R) (2003).

[8] H. Xu *et al.*, Phys. Rev. Lett. **85**, 716 (2000).

[9] E. Geraci *et al.*, Nucl. Phys. **A732**, 173 (2004).

[10] E. A. Uehling and G. E. Uhlenbeck, Phys. Rev. **43**, 552 (1933).

[11] E. J. Hellund and E. A. Uehling, Phys. Rev. **56**, 818 (1939).

[12] R. H. Anderson, C. J. Pethick, and K. F. Quader, Phys. Rev. B **35**, 1620 (1987).

[13] L. Shi and P. Danielewicz, Phys. Rev. C **68**, 064604 (2003).

[14] M. B. Tsang, Nucl. Phys. **A734**, 605 (2004).

[15] M. B. Tsang *et al.*, Phys. Rev. Lett. **92**, 062701 (2004).

[16] We note that the experimental impact parameter selection corresponds to rather peripheral collisions (estimated impact parameters $b/b_{\max} > 0.8$ fm [15]). In this sense the appropriate comparison should be with $t_c = 110$–120 fm/c interaction time simulations.

[17] M. Colonna *et al.*, Nucl. Phys. **A642**, 449 (1998).

[18] Ph. Chomaz, M. Colonna, and J. Randrup, Phys. Rep. **389**, 263 (2004).

[19] V. Baran, M. Colonna, and M. Di Toro, Nucl. Phys. **A730**, 329 (2004); E. De Filippo *et al.*, Phys. Rev. C **71**, 044602 (2005); **71**, 064604 (2005).

[20] M. Farine, T. Sami, B. Remaud, and F. Sebille, Z. Phys. A **339**, 363 (1998).

[21] F. Rami *et al.*, Phys. Rev. Lett. **84**, 1120 (2000).

[22] L. W. Chen, C. M. Ko, and Bao-An Li, Phys. Rev. Lett. **94**, 032701 (2005); A. W. Steiner and Bao-An Li, Phys. Rev. C **72**, 041601(R) (2005).

[23] R. Balian, *From Microphysics to Macrophysics*, Vol. II (Springer Verlag, Berlin, 1992).

[24] We note that this is also the mechanism behind the isospin distillation (n-enrichment of the gas phase) in the liquid-gas phase transition for asymmetric matter [3,4].

[25] R. Lionti *et al.*, Phys. Lett. **B625**, 33 (2005).